F-18-Labeled 3-Deoxy-3-Fluoro-D-Glucose for the Study of Regional Metabolism in the Brain and Heart

Mark M. Goodman, David R. Elmaleh, Kimberlee J. Kearfott, Robert H. Ackerman, Bernard Hoop, Jr., Gordon L. Brownell, Nathaniel M. Alpert, and H. William Strauss

Massachusetts General Hospital, Boston, Massachusetts

Glucose is the major physiological substrate of the brain and an important physiological substrate for the myocardium. [^{18}F]fluoro-3-deoxy-glucose [3-FDG(F-18)] was studied to determine whether it is a suitable tracer for evaluating the metabolic function of the brain and myocardium. 3-FDG(F-18) was rapidly accumulated in the mouse myocardium (10–12% injected dose/g) and remained constant up to 120 min. Blood, liver, and lung activities exhibited a rapid accumulation of activity (4% injected dose/g) at 1 min, followed by elimination of activity up to 30 min (2% injected dose/g), and then remaining unchanged for a period of 120 min. The arterial blood curve in the dog was fit best by three exponential components ($T_{1/2}$ = 0.52 min, 2.75 min, and 142.8 min). Transverse-section images were obtained of the dog's brain and myocardium. From sequential two-dimensional images, a clearance half-time of 26.88 min was determined for the canine brain. Radiation doses for man were calculated from tissue distribution data for mice.

J Nucl Med 22: 138–144, 1981

Transverse-section imaging of the brain and heart, using glucose analogs bearing positron-emitting radionuclides, has been found very valuable, since quantitative monitoring of the metabolism of the radiopharmaceutical may be obtained.

Glucose is the major energy source of the brain and is an important physiological substrate for the myocardium. Attempts have been made to utilize carbon-11 glucose ($T_{1/2}$ for C-11 = 20 min) as a radiotracer to measure the functional activity of the brain by quantitating the local cerebral glucose utilization with emission computed tomography (*1,2*). However, no attempts have been made to image the myocardium with C-11 glucose. Because of the rapid egress of C-11 (primarily as $^{11}CO_2$) from these tissues, no regional measurements of the brain or images of the heart have been reported. Recently, Ido et al. have synthesized an F-18-labeled analog of glucose (*3,4*) and its metabolic properties have been studied in detail (*5,6*). 2-(^{18}F)fluoro-2-deoxy-D-glucose [2-FDG(F-18)] has been used successfully to measure the functional activity of the brain (*7*), on the basis of the Sokoloff model development for 2-deoxy-D-[^{14}C] glucose (*8*) or on its improved version allowing for dephosphorylation of the trapped 2-FDG-PO_4 (F-18) (*9*). 2-FDG(F-18) has also been found a valuable tracer for imaging the myocardium and measuring relative metabolic changes in different circumstances (*10*). The synthesis of 2-(^{18}F)fluoro-2-deoxy-D-mannose [2-FDM (F-18)], an epimer of 2-FDG, has also been reported, and preliminary biodistribution studies in rats have shown that 2-FDM has biochemical properties similar to those of 2-FDG (*11*). To date, however, the syntheses of F-18 tagged 2-FDG and 2-FDM are possible only with a large cyclotron that has deuteron beam energy >6 MeV. Of the remaining fluorinated analogs of glucose, only the 3-fluoro-3-deoxy-D-glucose (3-FDG) derivative has been reported to have biochemical properties closely resembling those of glucose (*12*). A discussion of the selection of 3-FDG to measure local glucose metabolism has been recently published (*13*). 3-FDG is transported

Received March 3, 1980; revision accepted Aug. 29, 1980.

For reprints contact: David R. Elmaleh, Physics Research Lab., Massachusetts General Hospital, Boston, MA 02114.

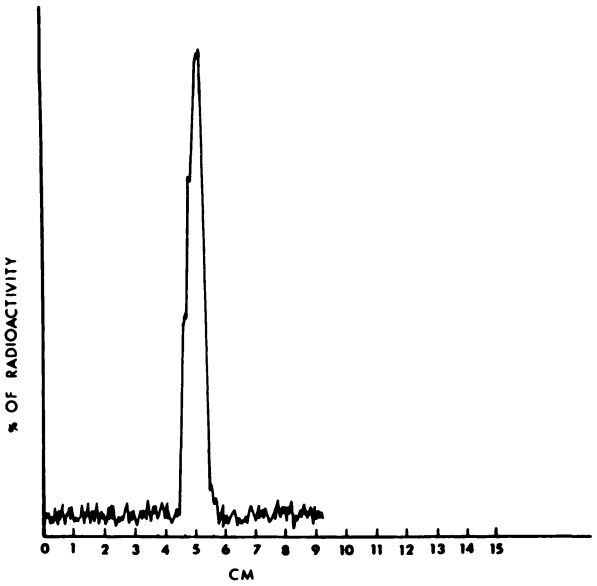

FIG. 1. High-pressure liquid chromatogram of 3-FDG(F-18), showing radioactivity profile. Column conditions: Lichrosorb-NH_2 column 30 cm by 0.4 cm, phosphate buffer, pH = 3.5, at 750 psi.

across mammalian membranes by the controlled processes of facilitated diffusion and active transport. In both processes the carbohydrate has been postulated to combine with a protein carrier to form a complex that carries the carbohydrate across the membrane (*14*). For the active transport model in the hamster intestine (*12*), 3-FDG was found to bind to the carrier just as effectively as D-glucose. For the facilitated diffusion model in the human erythrocyte (*15,16*) 3-FDG was again found to bind just as strongly to the carrier as D-glucose. Like glucose and 2-FDG, 3-FDG is a substrate for the enzyme hexokinase. It is not a very good one, however, for its Michaelis-Menten constant (K_m) = 70 ± 30 m*M* and its relative maximum velocity = 0.10, compared with those of D-glucose (K_m = 0.17 m*M* and relative maximum velocity = 1.00) and 2-FDG (K_m = 0.19 ± 0.03 m*M* and relative maximum velocity = 0.50) (*17*). The low affinity of 3-FDG for hexokinase may significantly affect the utilization of 3-FDG as a tracer for glucose metabolism in instances of high blood sugar, since 3-FDG would then compete with endogenous glucose for the substrate's active site.

Recently, a synthesis of 3-(^{18}F)fluoro-3-deoxy-D-glucose has been developed by Tewson and Welch (*18*), utilizing F-18 in a form that can be produced in a small medical cyclotron. A preliminary rectilinear scan of a rhesus monkey was reported (*13*), but with no animal biodistributions. We report our results with this glucose analog as a radiotracer for brain and heart studies. We investigated: (a) the biodistribution of 3-FDG in normal mice; (b) the time course of the distribution of 3-FDG in the brain, heart, and liver in normal mongrel dogs; (c) the arterial blood clearance; (d) the 2-D and 3-D images of the canine chest and head; and (e) the dosimetry of 3-FDG.

MATERIALS AND METHODS

The production of cesium radiofluoride ($Cs^{18}F$), almost carrier-free, has recently been reported (*13*). It was produced by the $^{20}Ne(d,\alpha)^{18}F$ reaction. Neon was bombarded with a 6.5-MeV deuteron beam directed onto a nickel-plated target box that is fitted with a self-contained Havar foil window. During bombardment the neon was circulated through a series of two silver-wool* plugs coated with cesium hydroxide. In a typical preparation, a 100-mg silver-wool plug was immersed in an aqueous cesium hydroxide solution (200 mg/ml) and dried at 150°C. Irradiation of the neon for 60 min at 40 μA beam current produces 60–65 mCi absorbed on the silver wool. Greater than 90% of the collected activity was trapped by the first silver plug. The reaction of a silver-wool plug containing $Cs^{18}F$ with 1,2:5,6 di-O-isopropylidene-O-trifluoromethane sulfonyl-D-cellofuranose gave 1,2:5,6 di-O-isopropylidene-3-deoxy-3-(^{18}F)fluoro-D-gluco-furanose, which was hydrolyzed to 3-FDG(F-18) as previously reported (*13*). In a typical experiment, a nitrogen-purged 0.5-ml solution of hexamethyl phosphoric triamide (HMPA) containing the silver-wool plug, and 25 mg of I, was heated in a sealed reaction vial at 140°C for 60 min. Less than 15% of the activity remained in the vial and on the silver. The isopropylidene groups of 1,2:5,6 di-O-isopropylidene-3-deoxy-3-(^{18}F)fluoro-2-D-gluco-furanose were removed by boron trichloride and water. The aqueous solution containing 3-FDG(^{18}F) was purified by passing the solution through a column consisting of alumina sandwiched between AG50X8 ion-exchange resin. The radiochemical purity was greater than 98% as determined by HPLC using the following conditions: Lichrosorb-NH_2 column, 30 cm long by 0.4 cm i.d., phosphate buffer, pH 3.5, at 750 psi. The radiochromatogram is shown in Fig. 1.

ANIMAL EXPERIMENTS

Mice. An aqueous solution of 3-FDG(F-18) was titrated with normal NaOH to pH 7.5 and sterilized by Millipore filtration (0.22 μm). The resulting solution was injected into CD-1 Fisher mice (Charles River strain) through a tail vein. At the desired time interval after injection, the mice were killed by cervical fracture. The organs and tissue samples were excised, rinsed, and blotted to remove adhering blood. The weighed organs were then counted in a well scintillation counter and the activity corrected for decay.

Dogs. Four mongrel dogs were anesthetized with sodium pentobarbital (Diabutol, 0.55 cc/kg) and the 3-FDG(F-18) (3–4 mCi) was injected through a femoral

TABLE 1. DISTRIBUTION OF FLUORINE-18 RADIOACTIVITY IN MOUSE TISSUES FOLLOWING I.V. INJECTION OF 3-FDG(F-18)

	% Injected dose/gram tissue (N = 5–6)				
	1 min	5 min	30 min	60 min	120 min
Blood	6.43 ± 0.80	5.70 ± 0.60	3.52 ± 0.48	2.14 ± 0.76	1.75 ± 0.44
Brain	4.00 ± 0.46	3.54 ± 0.71	2.14 ± 0.52	1.64 ± 0.27	2.03 ± 0.56
Liver	6.45 ± 0.95	5.83 ± 0.82	3.52 ± 0.34	2.26 ± 0.48	2.36 ± 0.62
Spleen	2.49 ± 0.44	2.45 ± 0.40	3.00 ± 0.38	2.08 ± 0.39	2.48 ± 0.73
Lung	4.69 ± 0.38	4.38 ± 0.66	3.78 ± 0.27	2.78 ± 0.54	3.12 ± 0.81
Heart	8.36 ± 1.52	7.32 ± 0.77	12.4 ± 2.13	10.1 ± 1.70	10.9 ± 2.06
Kidney	7.26 ± 1.18	5.43 ± 0.55	3.57 ± 0.38	2.18 ± 0.32	2.19 ± 0.58
Bone	2.45 ± 0.69	2.36 ± 0.40	2.69 ± 0.29	3.41 ± 0.50	3.50 ± 0.76
Muscle	2.32 ± 0.17	2.30 ± 0.68	2.90 ± 1.04	2.11 ± 0.18	2.30 ± 0.44
Bladder	1.23 ± 0.19		15.4 ± 19.4	4.73 ± 5.31	50.2 ± 31.9

vein. After a 10-sec injection of 3-FDG(F-18), serial blood samples were taken from a femoral arterial catheter to determine the blood clearance rate. A 3-cc aliquot was taken every 15 sec for 1 min, every 30 sec for the next 4 min, every minute for the next 10 min, every 15 min for the next 45 min, and every 30 min for the next 2 hr. The blood samples were weighed, counted in a well scintillation counter, and the activity corrected for decay.

2-D images. In order to determine the time course of the distribution of 3-FDG in the brain, heart, and liver, 2-D images of the dogs were made with the MGH positron camera PC-II. Before imaging, the dogs were placed between the camera heads, a phantom filled with an aqueous solution of F-18 ($T_{1/2}$ = 110 min) was placed beneath the dog, and a transmission image was taken. Four mCi of 3-FDG(F-18) were then administered i.v. into the normal dogs (weight ~15 kg) and 2-D lateral scans were made. After collection, the data were corrected for decay and photon attenuation.

3-D images. A set of positron emission images were collected at 30 equally spaced angles in a 180° sweep about the animal. A total of 180 two-dimensional images were collected in 18 min. From these data, 23 transverse-section images (corrected for random coincidences, photon absorption, and radioactive decay) were reconstructed at a resolution of 1.4 cm FWHM.

RESULTS

Distribution in mice. Table 1 shows the tissue distribution in mice at 1, 5, 30, 60, and 120 min for 3-(^{18}F)-fluoro-3-deoxy-D-glucose after i.v. injection. The accumulation of 3-FDG(F-18) is largest in the heart. The myocardial uptake reaches a maximum within 30 min and remains constant to 120 min. Lung and liver activities exhibited an elimination of 37 and 66%, respectively, at 120 min (Fig. 2), compared with their activities at 1 min. After 120 min, the heart-to-liver ratio was 4.4 and the heart-to-lung 3.5. The uptake in skeletal muscle differed dramatically from that in heart muscle (Fig. 3). Whereas the activity in the heart increased from 8.4 to 10.9%, the activity in the skeletal muscle remained essentially unchanged at 2.3%. The heart-to-blood ratio reached a maximum of 6.4 at 120 min. The accumulation of activity in bone showed a slow increase from 2.5%

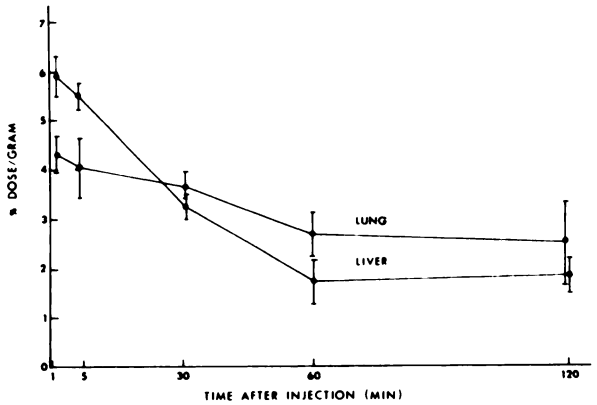

FIG. 2. Time course of radioactivity in lungs and liver of mice following i.v. injection of 3-FDG(F-18).

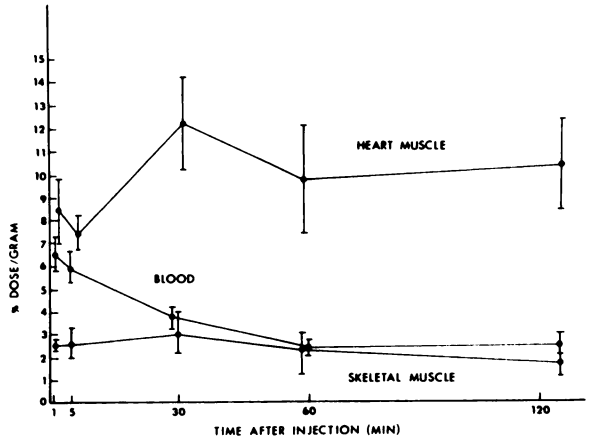

FIG. 3. Time course of radioactivity in heart muscle, skeletal muscle, and blood of mice after i.v. injection of 3-FDG(F-18).

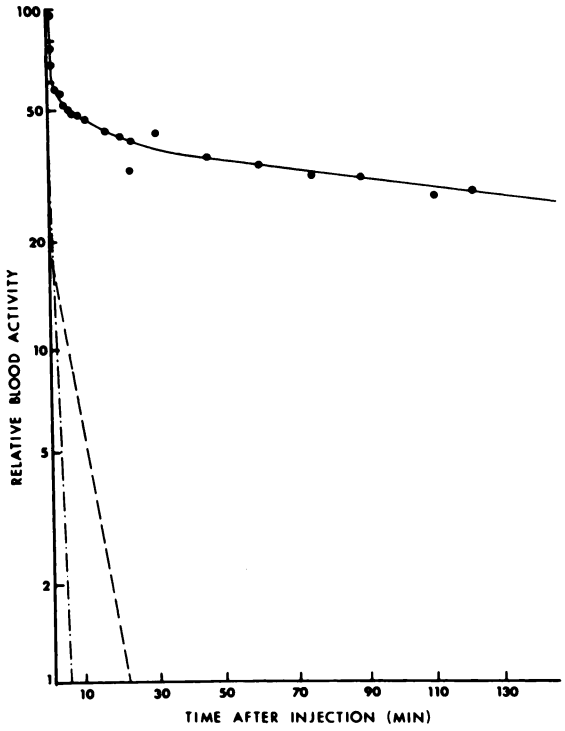

FIG. 4. Arterial blood curve in dog after i.v. injection of 3-FDG(F-18). Curve is average of four experiments.

at 1 min to 3.5% at 120 min. Thus, 3-(^{18}F)fluoro-3-deoxy-D-glucose does not appear to undergo defluorination easily. The brain exhibited a 49% elimination of activity from 1 to 30 min, and remained unchanged at 120 min.

Arterial blood clearance in dogs. Figure 4 shows the arterial blood curve for fluorine-18 following an i.v. injection of 3–4 mCi of 3-FDG in four dogs. This curve has been normalized to the largest available data point (0.25 min). Three exponentials fit the curve best; a major component with $T_{1/2}$ = 0.52 min, a slower one with 2.75 min, and a third with 142.8 min.

Tomographic studies. The tomographic images of a normal 15-kg dog, taken in PC-II, are shown in Figs. 5 and 6. The images of the head, Fig. 5, were taken after i.v. injection of 4.0 mCi of 3-FDG(F-18); there was a 5-min wait for blood clearance, then 18 min of data collection. Six consecutive cross-sectional slices of the head are illustrated. Each slice is 1.4 cm thick and corresponds to the numbered position shown in the 2-D image of the head. The dog's brain appears in slices 7, 7.5, 8, and 8.5, which, respectively, contain $10^6 \times 0.17$, 0.40, 0.24, and 0.48 counts. The images of the chest, Fig. 6, were taken after an i.v. injection of 4.0 mCi of 3-FDG(F-18) followed by 60 min for blood clearance and 18 min for data collection. Figure 6 shows the 3-

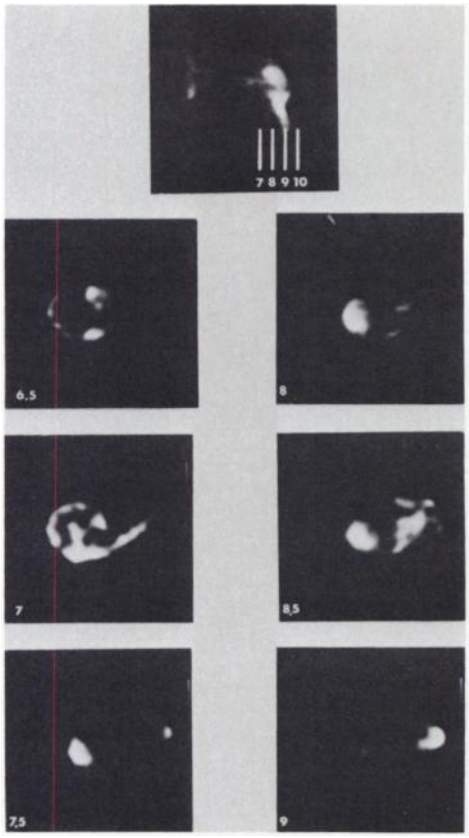

FIG. 5. Tomographic images of dog's head 5 min after i.v. injection of 3-FDG(F-18). Each 1.4-cm tomographic slice corresponds to position shown in 2-D lateral image (top).

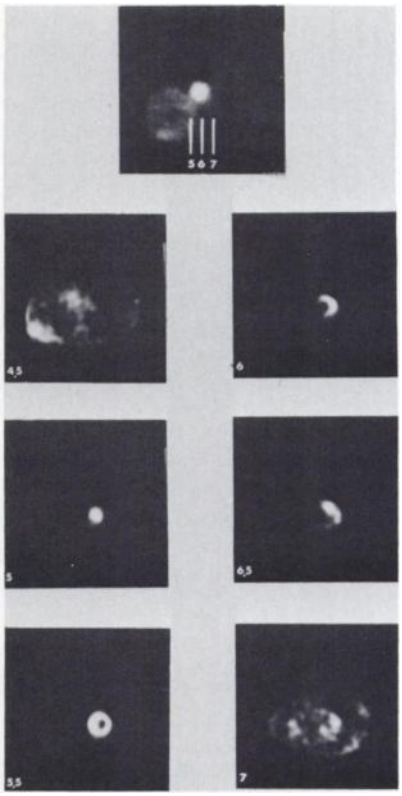

FIG. 6. Tomographic images of dog's chest 60 min after i.v. injection of 3-FDG(F-18). Each 1.4-cm tomographic slice corresponds to position shown in 2-D lateral image (top).

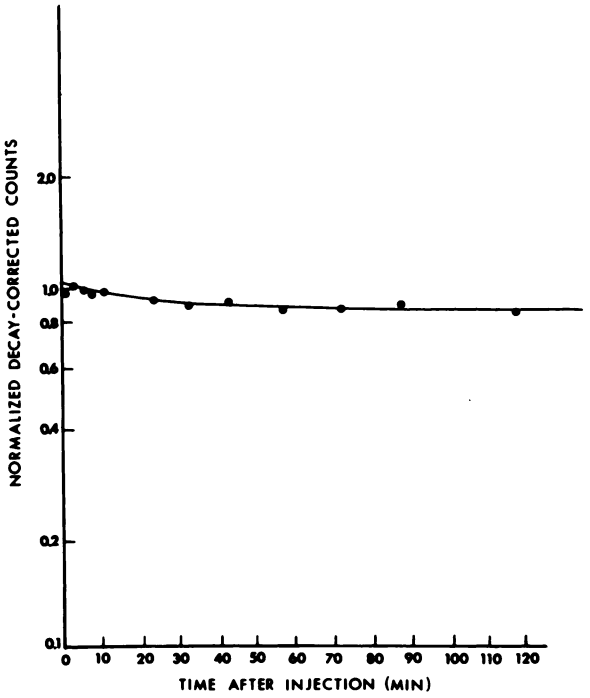

FIG. 7. Clearance of total radioactivity from dog's brain following injection of 3-FDG(F-18).

FDG(F-18) images of the myocardium in six consecutive cross sections. Each slice is 1.4 cm thick and corresponds to the position shown in the 2-D image of the chest. The left ventricle is clearly defined in slices 5, 5.6, and 6.5; they contain $10^6 \times 0.2$, 0.41, 0.19, and 0.29 counts.

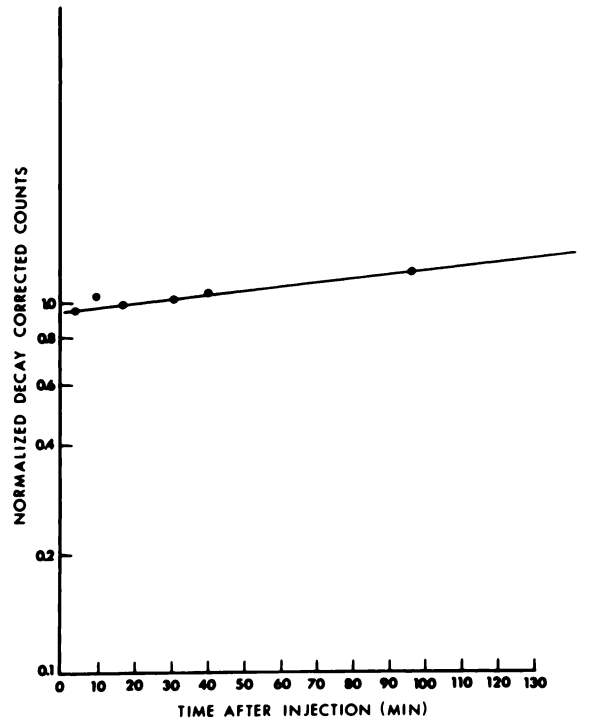

FIG. 8. Uptake of total radioactivity in dog's heart following injection of 3-FDG(F-18).

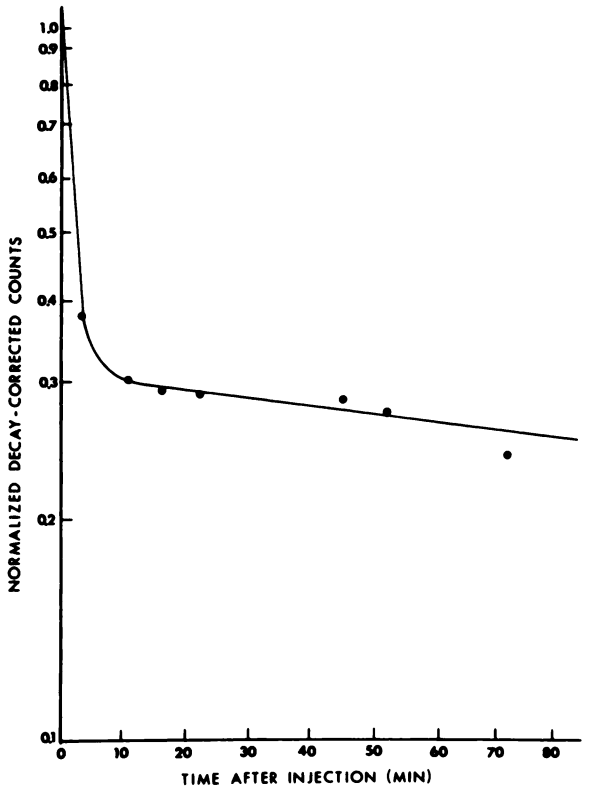

FIG. 9. Clearance of total radioactivity from dog's liver following injection of 3-FDG(F-18).

Time-activity studies. An important characteristic of a radiopharmaceutical is its selective accumulation and stability in the targeted tissue, and the rapid clearance from tissues that might mask the image. In the case of a metabolic trapping agent, such as 3-FDG, organ stability is very important, since the rapid egress of activity from the organ may hinder the quantification of the regional metabolism of the radiopharmaceutical. In order to determine the stability of 3-FDG in the brain and heart, several normal dogs were imaged repeatedly in a lateral position. Each time, the counts were totalled in the brain and heart and corrected for decay and attenuation. The data were then normalized and plotted as a function of time. Figure 7 shows thirteen brain-activity data points from 2 to 180 min. A single exponential component fitted the curve best. The component had a half-time of 26.88 min and fitted the data to within 4.4% for times greater than 2 min. These results indicate a rapid uptake with a subsequent slow net leakage to a constant value.

The F-18 distribution in the myocardium is shown in Fig. 8, with cardiac data points taken from 2 to 90 min. The data indicate a slow uptake with a 5.1-hour half-time. Heart-to-liver ratio increased from 0.97 at 3 min to 1.60 at 90 min (Fig. 9).

Dosimetry. The radiation dose for 3-FDG(F-18) in man was estimated using tissue distribution data from mice. Since the time course of organ distribution has

TABLE 2. DISTRIBUTION OF FLUORINE-18 RADIOACTIVITY IN MOUSE TISSUES FOLLOWING I.V. INJECTION OF 3-FDG(F-18)

	% Injected dose/organ (N = 5–6)				
	1 min	5 min	30 min	60 min	120 min
Blood	15.847 ± 1.929	15.744 ± 1.250	9.668 ± 1.278	5.131 ± 1.815	4.198 ± 1.049
Brain	1.508 ± 0.149	1.548 ± 0.433	1.027 ± 0.286	0.703 ± 0.171	0.823 ± 0.208
Liver	10.609 ± 1.333	10.922 ± 2.746	7.118 ± 0.726	4.405 ± 0.523	3.834 ± 0.939
Spleen	0.259 ± 0.045	0.277 ± 0.085	0.345 ± 0.075	0.220 ± 0.040	0.316 ± 0.037
Lung	0.768 ± 0.062	0.828 ± 0.071	0.684 ± 0.049	0.585 ± 0.084	0.674 ± 0.119
Heart	0.789 ± 0.088	1.004 ± 0.082	1.552 ± 0.132	1.704 ± 0.281	1.203 ± 0.221
Kidney	3.177 ± 0.327	3.186 ± 0.323	1.944 ± 0.159	1.285 ± 0.160	1.146 ± 0.286
Bone	7.482 ± 1.955	8.666 ± 1.275	9.320 ± 1.296	10.108 ± 2.477	10.504 ± 2.273
Muscle	32.229 ± 2.802	36.925 ± 11.755	44.748 ± 15.782	28.505 ± 2.403	39.010 ± 5.942
Bladder	0.081 ± 0.013		0.486 ± 0.467	0.166 ± 0.113	7.182 ± 5.852

been determined, the cumulative dose for each organ could be calculated.

The organ distribution of 3-FDG(F-18) in mice at 1, 5, 30, 60, and 120 min is shown in Table 2. Least-square exponential fits were done to estimate the biological half-time.

Using these data a cumulative activity (μCi-hr) for each organ was obtained. The radiation dosimetry was then obtained by using the dose calculational scheme of MIRD Pamphlet No. 11 (1975). The effective half-times and accumulated activities for the radiopharmaceutical in the source organs are included in Table 3. These numbers include the 110-minute physical half-life for F-18. Table 4 shows the best estimate of dose to humans per 1 mCi of 3-FDG(F-18) injected. Doses for a typical 5-mCi injection are also included.

DISCUSSION

The time-activity studies have shown that 3-FDG(F-18) enters the dog's brain and heart rapidly; this is followed by a gradual increase ($T_{1/2}$ = 306 min) in the heart and a slow release ($T_{1/2}$ = 26.88 min) from the brain. Following an i.v. injection, the concentration of 3-FDG(F-18) in the brain, heart, liver, lungs, and blood of dogs was initially high. However, the activity in the blood, liver, and lungs showed a rapid clearance in both dogs and mice. The canine arterial blood clearance of 3-FDG(F-18) was rapid, with $t_{1/2}$ = 0.52 min and 2.75 min for the fast components. This compares favorably with $t_{1/2}$ = 0.54 min and 5.92 min for the fast components of 2-FDG(F-18) (*2*). The slowest component, however, is slower in 3-FDG(F-18) than in 2-FDG(F-18): $t_{1/2}$ = 142.8 compared with 80.4 min. One possible explanation for this difference may lie in the relative affinities of 3-FDG (K_m = 70 ± 30 m*M*, V_{max} = 0.10) and 2-FDG (K_m = 0.19 ± 0.03 m*M*, V_{max} =

TABLE 3. ACCUMULATED ACTIVITIES AND EFFECTIVE HALF-TIMES FOR VARIOUS ORGANS COMPUTED BY MIRD #11 FOR MGH 3-FDG BIODISTRIBUTION IN NORMAL MICE

Organ	$\tilde{A}$ (μCi-hr)	Eff $t_{1/2}$ (min)
Brain	41.1	60.8
Thyroid	2.32	54.6
Heart	63.7	57.0
Lungs	70.8	85.4
Liver	176.0	44.5
Pancreas	7.04	48.2
Spleen	5.4	32.5
Kidneys	52.4	46.0
Bladder	37.0	103.0
Blood	197.0	37.1
Stomach	28.7	54.1
Skeleton	50.5	103.0

TABLE 4. HUMAN DOSE PER mCi ADMINISTERED 3-FDG(F-18), EXTRAPOLATED FROM BIODISTRIBUTION IN NORMAL MICE

Organ	Total dose (mrad/mCi)	Doses for 5 mCi injection (mrad)
Brain	16	80
Thyroid	182	910
Heart	63	315
Lungs	94	470
Liver	135	675
Pancreas	99	495
Spleen	73	365
Kidneys	168	840
Ovaries	52	260
Uterus	52	260
Blood	51	255
Skin	37	185
Stomach	92	460
Skeleton	53	265
Whole body	71	355

0.50) for the enzyme hexokinase. Since 3-FDG and 2-FDG have similar affinities for the carrier that transports these substrates across tissue membranes (*7*), the differences in blood clearance may depend on the relative rates of the reaction with hexokinase. 2-FDG has been shown to be a good substrate for this enzyme, whereas 3-FDG is a poor one (*17*). An alternative explanation for the slow blood clearance of 3-FDG is the reabsorption of 3-FDG from the glomerular filtrate in the kidneys back into the blood. Glucose is returned to the blood mainly by way of an active transport mechanism in the renal tubules. For the active transport model in the hamster intestine (*12*), 3-FDG (K_i = 2.5 m*M*) was found to bind to the protein carrier just as effectively as D-glucose (K_i = 2.3 m*M*), whereas 2-FDG did not undergo active transport (*12*). Therefore, reabsorption in the kidneys can occur with 3-FDG but should not occur with 2-FDG.

The myocardial and cerebral tomograms obtained with 3-FDG(F-18) showed high accumulation of the tracer in these tissues. The left ventricle of the dog's myocardium was clearly visualized following a 4-mCi injection. Meanwhile, the activity in the liver and lungs—organs that might interfere with myocardial imaging—underwent substantial clearance and were not visible 90 min after injection. The brain was clearly visualized without interference from surrounding tissues, such as the skull. However, due to the small size of the dog's brain, tomograms showing fine structures were not obtained.

The rapid accumulation and slow release of 3-FDG(F-18) in the brain and myocardium, combined with the rapid clearance from the blood, demonstrate that 3-FDG(F-18) possesses properties similar to those of 2-FDG, and might be a suitable tracer for imaging and measuring the local glucose metabolism in the brain and heart.

FOOTNOTE

* Fisher Scientific

REFERENCES

1. RAICHLE ME, LARSON KB, PHELPS ME, et al: In vivo measurement of brain glucose transport and metabolism employing glucose-^{11}C. *Am J Physiol* 228:1936-1948, 1975
2. RAICHLE ME, WELCH MJ, GRUBB RL, et al: Measurement of regional substrate utilization rates by emission tomography. *Science* 199:986-987, 1978
3. IDO T, WAN C-N, FOWLER J, et al: Fluorination with F_2. A convenient synthesis of 2-deoxy-2-fluoro-D-glucose. *J Org Chem* 42:2341-2342, 1977
4. IDO T, WAN C-N, CASELLA V, et al: Labeled 2-deoxy-D-glucose analogs ^{18}F-labeled 2-deoxy-2-fluoro-D-glucose analogs ^{18}F-labeled 2-deoxy-2-fluoro-D-glucose, 2-deoxy-2-fluoro-D-mannose and ^{14}C-2-deoxy-2-fluoro-D-glucose. *J Label Comp Radiopharm* 14:175-183, 1978
5. GALLAGHER BM, ANSARI A, ATKINS H, et al: Radiopharmaceuticals XXVII ^{18}F-labeled 2-deoxy-2-fluoro-D-gluclose as a radiopharmaceutical for measuring regional myocardial glucose metabolism in vivo: Tissue distribution and imaging studies in animals. *J Nucl Med* 18:990-996, 1977
6. GALLAGHER BM, FOWLER JS, GUTTERSON NI, et al: Metabolic trapping as a principle of radiopharmaceutical design: some factors responsible for the biodistribution of [^{18}F] 2-deoxy-2-fluoro-D-glucose. *J Nucl Med* 19:1154-1161, 1978
7. REIVICH M, KUHL D, WOLF A, et al: The [^{18}F]fluorodeoxyglucose method for the measurement of local cerebral glucose utilization in man. *Circ Res* 44:127-137, 1979
8. SOKOLOFF L, REIVICH M, KENNEDY C, et al: The [^{14}C]deoxyglucose method for the measurement of local cerebral glucose utilization: Theory, procedure, and normal values in the conscious and anesthetized albino rat. *J Neurochem* 28:897-916, 1977
9. PHELPS ME, HUANG SC, HOFFMAN EJ, et al: Tomographic measurement of local cerebral glucose metabolic rate in humans with (F-18)2-fluoro-2-deoxy-D-glucose: Validation of method. *Ann Neurol* 6:388, 1979
10. PHELPS ME, HOFFMAN EJ, SELIN C: Investigation of [^{18}F]2-fluoro-2-deoxyglucose for the measured myocardial glucose metabolism. *J Nucl Med* 19:1311-1319, 1978
11. ROBINSON GD, PHELPS ME, HUANG SC: F-18-2-deoxy-2-fluoro-D-mannose: Biological behavior compound with 2-deoxy-2-fluoro-D-glucose *J Nucl Med* 20:672, 1979 (abst)
12. BARNETT J: Fluorine as a Substituent for Oxygen in Biological Systems: Examples in Mammalian Membrane Transport and Glucosidase Action. Carbon-Fluorine Compounds Chemistry, Biochemistry and Biological Activities: a CIBA Foundation Symposium, Amsterdam, Associated Scientific Publishers, 1972, pp. 95-115
13. TEWSON TJ, WELCH MJ, RAICHLE ME: [^{18}F]-labeled 3-deoxy-3-fluoro-D-glucose: Synthesis and preliminary biodistribution data. *J Nucl Med* 19:1339-1345, 1978
14. LEHNINGER AL: *Biochemistry*. 1st ed., New York, Worth Publishers, Inc. 1970, pp 605-627
15. BARNETT JE, HOLMAN GD, MUNDAY KA: Structural requirements for binding to the sugar-transport system of the human erythrocyte. *Biochem J* 135:773-777, 1973
16. RILEY GJ, TAYLOR NF: The interaction of 3-deoxy-3-fluoro-D-glucose with the hexose-transport system of the human erytyrocyte. *Biochem J* 135:773-777, 1973
17. BESSELL EM, FOSTER AB, WESTWOOD JH: The use of deoxyfluoro-D-glucopyranoses and related compounds in a study of yeast hexokinase specificity. *Biochem J* 128:199-204, 1972
18. TEWSON TJ, WELCH MJ: New approaches to the synthesis of 3-deoxy-3-fluoroglucose. *J Org Chem* 43:1090, 1978